Estimation of the effect of methane content variations on the radiation balance in the Earth–atmosphere system

L.I. Kurbatskaya

Institute of Computational Mathematics and Mathematical Geophysics, Novosibirsk

Received February 12, 2001

The effect of variations of methane concentration on the radiation budget (IR radiation, radiation balance on the Earth's surface) and, as a consequence, variations of the intensity of methane emissions are considered. Some results are presented that demonstrate the effect of variations of methane concentration on radiation budget.

In this paper, we assess the effect of the trace gas methane (CH_4) in the Earth's atmosphere on the mesoclimate. As an absorber of IR radiation, methane follows the carbon dioxide (CO_2). Here we consider the effect of variations in the methane concentration on the radiation budget (IR radiation, radiation balance on the Earth's surface). The results are presented that demonstrate the effect of variations in the methane concentration on the radiation budget of the Earth–atmosphere system.

Minor gaseous constituents of the atmosphere actively absorb IR radiation. As known carbon dioxide, CO_2, plays an important part (the second after water vapor) in the radiation budget. Carbon dioxide is well mixed in the atmosphere, its concentration increases from year to year, and now it is 345 ppmv. In recent years, a significant attention has been paid to the problem of the CO_2 concentration growth in the atmosphere due to anthropogenic factors, because the qualitative analysis of consequences from this growth allows the conclusion to be drawn on the intensification of the greenhouse effect causing global warming.

The methane gas CH_4 is the next, in significance, absorber of IR radiation. Before passing to consideration of the absorption of IR radiation by the methane, let us briefly characterize this gas.[1]

Methane CH_4 is a carbonic component, which is generated near the Earth's surface and is gradually transported aloft up to the heights, where it is oxidized thus becoming a source of carbon monoxide and formaldehyde. There are no chemical sources of CH_4 in the atmosphere; it is generated in the biosphere and lithosphere. Vital activity of anaerobic bacteria contributes significantly to biological generation of methane. These bacteria exist in the alkaline medium at rather high temperatures and abundant organic matter. Such a medium is typical of marches, large ponds, and rice plantations. Table 1 (Ref. 1) gives the estimates of the methane amounts produced annually by the above-listed sources.

The total amount of generated methane yields the vertical flow $2.5 \cdot 10^{-11}$ cm^{-2}·s^{-1} and the mean lifetime of 4–10 years. These data allow us to estimate the total amount of methane in the atmosphere as 4600 Mt. The vertical distribution of methane is determined by the equilibrium between its destruction in chemical reactions and upward transport from the surface.

Table 1

Source	Methane amount, Mt/year
Natural waterlogged zones (marches, ponds, etc.)	200–300
Rice plantations	140–280
Animal fermentation	100–200
Tundra, ocean and lake shores	3–50
Biological sources on the whole	443–850
Industrial emissions	16–50
Fuel burning	0–160
Anthropogenic sources on the whole	16–210

The main sink of methane in the atmosphere is the reaction with OH hydroxyl, and the rest part is accumulated in the atmosphere. According to Ref. 2, the total level of methane sink and accumulation in the atmosphere is (495 ± 145) Mt/year. In this sum, the atmospheric sink in reactions with OH is (425 ± 125) Mt/year. Absorption by soil is estimated as (10 ± 5) Mt/year; this value is far lower than the yearly accumulation of methane in the atmosphere that equals (60 ± 15) Mt/year. Based on these estimates, we can assume that methane to be subject to the action of two factors: ecological (participation in chemical reactions producing, for example, formaldehyde) and climatic (absorption of IR radiation in the atmosphere).

Nowadays the concentration of methane in the atmosphere is ≈ 1.7 ppmv. Methane is well mixed in the troposphere, but, above the tropopause, its concentration decreases quickly due to oxidation and participation in reactions with other gases. The methane content gradually increases, by 1.2–1.5%, from year to year. The latitudinal distribution of the annually mean methane concentration grows from the equator to the pole (in the Northern Hemisphere), and in the high latitudes the methane concentration increases sharply in fall due to the growth of emissions from swampy soil

0235-6880/01/06–07 489-04 $02.00

rich in water. It should be noted that the methane concentration, on the average, is roughly 200 times lower than the concentration of CO_2. Nevertheless, here we consider the problem of the allowance for methane when calculating the radiation characteristics (upwelling and downwelling fluxes of longwave radiation, radiant cooling rate, and radiation balance on the Earth's surface and at the top of the atmosphere) and estimate the effect of methane variations on the IR radiation, which possibly can intensify the greenhouse effect. Besides, we compare this effect with the effect of CO_2, whose role in the greenhouse effect is unquestionable.

For this purpose, we use the radiation model of the plane-parallel atmosphere being in the local thermodynamic equilibrium. The equations for the up and downwelling fluxes are written as[3]

$$F_i(p)^{\uparrow} = [B_i(g) - B_i(p_s)]\,T_i(p, p_s) + B_i(p) - \int_{p_s}^{p} T_i(p, p')\,[\mathrm{d}B_i(p')/\mathrm{d}p]\,\mathrm{d}p', \quad (1)$$

$$F_i(p)^{\downarrow} = [B_i(top) - B_i(p_{top})]\,T_i(p, p_{top}) + B_i(p) + \int_{p}^{p_{top}} T_i(p, p')\,[\mathrm{d}B_i(p')/\mathrm{d}p]\,\mathrm{d}p', \quad (2)$$

$$F_{i,\mathrm{net}} = F_i(p)^{\uparrow} - F_i(p)^{\downarrow};$$

$$H(p) = (g_0/C_p)\,\mathrm{d}\Big[\sum_i F_{i,\mathrm{net}}(p)\Big]/\mathrm{d}p.$$

Here $F(p)^{\uparrow}$ and $F(p)^{\downarrow}$ are the up and downwelling fluxes for the ith spectral interval; $B_i(p)$ is the Planck's function; p_s is the pressure on the Earth's surface; p_{top} is the pressure at the top of the atmosphere; $T_i(p, p')$ is the transmission function for the layer from p to p'; g denotes the ground level; *top* means the top of the atmosphere; g_0 is the acceleration due to gravity ($g_0 = 9.807$ m/s^2, $C_p = 1004$ J/(kg · deg)); $H(p)$ is the radiant cooling rate.

It should be noted that the effective flux $F_{i,\mathrm{net,s}} = F_i(p_s)^{\uparrow} - F_i(p_s)^{\downarrow}$ on the Earth's surface corresponds to the black body condition, $F_i(p_s)^{\uparrow} = \sigma T_s^4$. Under actual conditions, the upwelling longwave (thermal) radiation flux at the surface level is a sum of two parts: radiation emitted by surface, $\delta\sigma T_s^4$ and a fraction of downwelling radiation reflected by the surface $(1 - \delta)\,F_i(p_s)^{\downarrow}$. Here δ is the emissivity. The value $\delta = 1$ corresponds to the idealized limiting case. This case is considered here because the effect of methane on longwave flux as compared with the effect of other gaseous components (H_2O, CO_2) was estimated with the use of the radiation model constructed for the case of $\delta = 1$.

The transmission function is written as

$$T_i(p, p') \cong \exp\left\{ -\frac{\bar{S}_i\,u}{\sigma_i}\left(1 + \frac{\bar{S}_i\,u}{\pi\alpha}\right)^{-1/2}\right\}, \quad (3)$$

where $\bar{S}_i$ is the intensity of the ith line; σ_i is the distance between the lines; α is the Lorentz halfwidth; u is the optical path length along the vertical direction.

The transmission function $T_i(p, p')$ depends on three parameters: $\bar{S}_i/\sigma_i$, α, and u. The optical path length is determined as

$$u = \int_z^{\infty} \rho_k\,\mathrm{d}z, \quad (4)$$

where ρ_k is the density of the considered gas. The parameters $\bar{S}_i/\sigma_i$ and α are given in Table 2 as borrowed from Ref. 4 and complemented with the data on CH_4 from Ref. 5.

Table 2. Parameters of the statistical model of a band in the IR region for CH_4 (band at 6–9.2 μm)

Interval, cm^{-1}	$\bar{S}_i/\sigma_i$, cm^2·g^{-1}	$\pi\alpha/\sigma_i$
1180–1240	90.4	0.17
1240–1300	1325.9	0.24
1300–1360	2800.1	0.28
1360–1420	109.4	0.39
1420–1680	10.9	0.14

The radiation model is constructed in the following way. Within each spectral interval of the considered absorption band, the transmission function $T_i(p, p')$ is calculated for water vapor and methane according to Eq. (3); this function is then used in Eqs. (1) and (2) to determine the upward and downward fluxes. Along the vertical, a 15-level model with the given boundary conditions at the top and bottom of the atmosphere is considered.

The radiation model from Ref. 6 accounts for 17 spectral intervals, five of which fall within the H_2O (and CH_4) absorption band at 1180–1680 cm^{-1}. This band is called the H_2O rotational-vibrational 6.3-μm band.

The contribution of this band to the total radiant cooling is small as compared with those from other bands. Table 3 gives the radiant cooling rates for this absorption band with methane variations at unchanged water vapor content. The last column of Table 3 gives the total radiation cooling rates $\partial T/\partial t$ for the spectral intervals falling within the absorption bands to the left (0–1180 cm^{-1}) and to the right (1680–2000 cm^{-1}) from the considered band. They remain unchanged for all experiments with methane variations. It should be noted that the radiant cooling rates $\partial T/\partial t$ in the absorption bands to the left and to the right from the band of absorption by H_2O and CH_4 are caused by absorption of such gases as water vapor, carbon dioxide, and ozone.

The experiments have been conducted using the data of the standard altitude distribution of temperature, specific humidity, and pressure. The volume content of carbon dioxide and ozone was constant in the experiments, and the methane content was strongly varied from the real distribution.

The effect of minor gases on the longwave radiation was considered in Ref. 6. To estimate the

effect of methane in the 1180–1680 cm^{-1} absorption band, the following variants have been considered:

1. {H_2O}; 4. {H_2O} + 4·{CH_4};
2. {H_2O} + {CH_4}; 5. {H_2O} + 8·{CH_4};
3. {H_2O} + 2·{CH_4}; 6. {H_2O} + {CO_2},

where braces are used for the concentration of the corresponding gas. Denote the variation of the methane concentration as δ{CH_4}.

In the absence of methane, the total radiant cooling rate would be the sum of the first and the last columns of Table 3. Other columns describe the radiant cooling rates for different δ{CH_4}. It is seen from Table 3 that every succeeding variation of the methane concentration decreases the radiant cooling rate in the lower troposphere. Although this decrease makes up only hundredths degree, the greenhouse effect nevertheless takes place.

Table 3. Radiation cooling rate $\partial T/\partial t$ (°C/day) for {H_2O} with variations of CH_4 concentration as a function of p

$\partial T/\partial t$ / p, mbar	H_2O	H_2O + + CH_4	H_2O + + $2CH_4$	H_2O + + $4CH_4$	H_2O + + $8CH_4$	H_2O + + CO_2
0	0	0.004	0.005	0.006	0.006	−0.571
51.0	0	0.012	0.016	0.021	0.024	−0.257
105.0	0.005	0.023	0.030	0.038	0.046	−0.377
164.0	−0.029	−0.104	−0.004	0.001	0.005	−1.111
229.0	−0.128	−0.114	−0.111	−0.109	−0.108	−2.241
300.0	−0.168	−0.161	−0.159	−0.158	−0.156	−2.306
378.0	−0.153	−0.150	−0.148	−0.146	−0.143	−1.800
463.0	−0.164	−0.162	−0.158	−0.151	−0.141	−1.461
551.0	−0.444	−0.452	−0.453	−0.451	−0.446	−2.122
642.0	−0.233	−0.216	−0.205	−0.190	−0.173	−1.200
732.0	−0.244	−0.219	−0.207	−0.192	−0.174	−1.233
817.0	−0.194	−0.173	−0.162	−0.149	−0.134	−1.074
893.0	−0.209	−0.192	−0.183	−0.172	−0.158	−1.103
979.0	−0.255	−0.228	−0.214	−0.197	−0.176	−1.307
1010.0	−0.641	−0.583	−0.556	−0.524	−0.486	−3.169

It is seen from Table 4 that if gases are absent, the Earth longwave radiation reaches the top of the atmosphere without changes. The atmosphere is not cooled due to radiant cooling. Every next row of Table 4 describes the behavior of the above-listed radiation characteristics depending on δ{CH_4} at the unchanged water vapor content. The longwave radiation is absorbed by water vapor within the entire absorption band from 40 to 2200 cm^{-1}. Every succeeding variation of the methane concentration changes the surface radiation balance that is caused by the longwave radiation. The variation of the value of $(F_s^{\downarrow} - \sigma T_s^4)$ manifests itself already at the real distribution of the mean methane concentration. The two-fold, four-fold, eight-fold and more increase of the mean methane concentration with respect to the real distribution causes further change of this value. It is seen that the variation of $(F_s^{\downarrow} - \sigma T_s^4)$ does not follow a linear dependence. The same conclusions are valid for other characteristics, such as the upward flux at the top of the atmosphere $F_{\infty}^{\uparrow}$ and the radiant cooling rate $\partial T/\partial t$ for the atmospheric layer with the thickness ΔP. It is also seen from Table 4 that the listed radiation characteristics mostly depend on the presence of water vapor and carbon dioxide in the atmosphere. In the absence of water vapor, the major contribution is due to carbon dioxide.

Table 4. Downwelling $F_S^{\downarrow}$ and upwelling $F_{\infty}^{\uparrow}$ fluxes, longwave radiation balance on the surface $(F_s^{\downarrow} - \sigma T_s^4)$, and radiant cooling rates $\partial T/\partial t$ for the atmospheric layer with the thickness $\Delta P = (P_s - P_{\infty}) = 1013$ mbar for H_2O with variations of methane and CO_2

Gaseous constituents and their variations	$F_s^{\downarrow}$, $W \cdot m^{-2}$	$F_{\infty}^{\uparrow}$, $W \cdot m^{-2}$	$(F_s^{\downarrow} - \sigma T_s^4)$, $W \cdot m^{-2}$	$\partial T/\partial t$, °C/day
Gaseous constituents are absent	0.0	461.02	−461.02	0.0
H_2O	287.79	351.72	−173.23	−1.487
$H_2O + CH_4$	288.76	349.25	−172.26	−1.470
$H_2O + 2 \cdot CH_4$	289.24	348.02	−171.78	−1.468
$H_2O + 4 \cdot CH_4$	289.86	348.47	−171.16	−1.460
$H_2O + 8 \cdot CH_4$	290.62	344.62	−170.62	−1.451
$H_2O + 16 \cdot CH_4$	291.68	342.54	−169.54	−1.441
CO_2	76.65	384.37	−409.70	−0.210
$H_2O + CO_2$	319.65	309.60	−141.37	−1.401
$H_2O + 2 \cdot CO_2$	321.58	304.71	−139.44	−1.377
$H_2O + CO_2 + CH_4$	320.62	307.14	−140.40	−1.389

The modeling results obtained in this paper are intercompared in Table 5 with the results of Refs. 8 and 9. The table consists of three parts: A, B, and C. Part A of Table 5 gives the results of Ref. 8 (case 37a). The data in Ref. 8 have been obtained from the results of 11 radiation models, which accounted only for the effect of methane with the concentration not changing with height and equal to 1.75 ppmv. The calculations have been performed with the use of the midlatitude summer model of the atmosphere. This atmospheric model determines the altitude (z) distribution of pressure p, air temperature T, water vapor density ρ_{H_2O}, ozone density ρ_{O_3}, and air density ρ. From the results of 11 models, mean values of the upward, downward, and effective fluxes on the surface and at the height of the tropopause have been determined. The upward fluxes at the top of the atmosphere have been found, the difference for the effective flux at the height of the tropopause and on the surface, as well as the difference of the upward flux at the top of the atmosphere and the effective flux at the tropopause level, has been presented. The second row of Part A gives the standard deviations for all the above-listed characteristics, and the third row gives the maximum spread in values.

The results of this work are presented in Part B of Table 5. The calculations have been made using the same model of the atmosphere (midlatitudes, summer). It is seen from Table 5 that the obtained characteristics agree well with the statistical (over 11 models) results from Ref. 8.

Table 5

	Parameters	Earth's surface			Tropopause			Top of the atmosphere		
		$F_s^{\uparrow}$	$F_s^{\downarrow}$	$F_{net,s}$	$F_{tr}^{\uparrow}$	$F_{tr}^{\downarrow}$	$F_{net,tr}$	$F_{net,top}$	$(F_{net,tr} - F_{net,S})$	$(F_{top}^{\uparrow} - F_{net,tr})$
A	Ref. 8									
	Mean	423.23	7.45	415.77	418.46	0.23	418.23	417.96	2.46	−0.26
	Standard dev.	0.81	2.02	2.20	1.12	0.06	1.13	1.14	1.84	0.07
	Spread in values	3.12	7.87	7.73	3.71	0.22	3.86	3.84	6.61	0.26
	Number of models	11	11	11	11	11	11	11	11	11
B	This model	423.02	7.47	415.55	417.35	0.26	417.06	416.75	2.54	−0.35
C	Ref. 9: Methane concentration, ppmv									
	1.75		6.94			0.32			–	
	3.50		9.86			0.47			–	
	This model: Methane concentration, ppmv									
	1.75		7.47			0.26			–	
	3.50		10.15			0.49			–	

Part C of the Table 5 presents the results of Ref. 9 and this work for the methane concentration equal to 1.75 ppmv and the doubled methane concentration equal to 3.50 ppmv. The comparison shows that the longwave radiation fluxes calculated in this work using the model allowing for the effect of methane well agree with the corresponding fluxes estimated in Ref. 9.

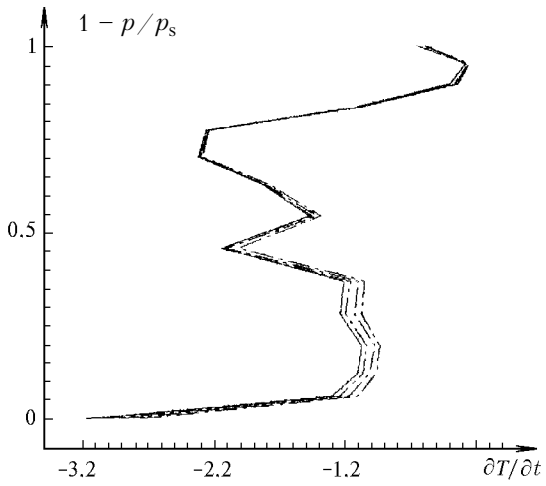

Fig. 1. Radiant cooling rate as a function of methane variations.

Figure 1 shows the dependence of the radiant cooling rate $\partial T/\partial t$ (in °C/day) on the methane variations. The vertical coordinate is a dimensionless variable $(1 - p/p_s)$, where p is the current pressure, and p_s is the pressure on the surface. The solid curve corresponds to the radiant cooling rate neglecting methane. The dashed curves describe the effect of methane as its concentration increases 10 and 100 times. From Fig. 1, as well as from Table 4, it is seen that as the methane concentration in the atmosphere increases, the cooling rate in the lower troposphere decreases.

The numerical experiments with the methane variations have shown that in the climatic aspect the increase of the methane concentration leads to a slight decrease of cooling in the atmosphere. However, due to the increase of the methane concentration, the extra energy caused by the longwave radiation of the atmosphere reaches the surface. This may change emission of methane from marches. We can also assume that if the methane emission is significant and swampy territories are vast, and then climatic consequences may be noticeable. However, for this to take place, the methane concentration must increase by 20 times, at least.

Acknowledgments

The work was partially supported by Grant "Leading Scientific Schools" No. 00–15–98543, Russian Foundation for Basic Research Grant No. 01–05–65313, and the Integration Grant SB RAS–2000 No. 64, 73.

References

1. N.M. Bazhin, Khimiya v Interesakh Ustoichivogo Razvitiya **1**, No. 3, 381–397 (1993).
2. G. Brasseur and S. Solomon, *Aeronomy of the Middle Atmosphere* (D. Reidel Publishing Company, Dordrecht, 1984).
3. M.A.K. Khalil and R.A. Rasmusson, J. Geophys. Res. C **88**, No. 9, 5131–5144 (1983).
4. W.T. Roach and A.A. Slingo, Quart. J. R. Meteorol. Soc. **105**, No. 445, 603–615 (1979).
5. K.N. Liou, *An Introduction to Atmospheric Radiation* (Academic Press, New York, 1980).
6. E.V. Rozanov, Yu.M. Timofeev, and V.A. Frol'kis, Izv. Akad. Nauk SSSR, Ser. Fiz. Atmos. Okeana **17**, No. 4, 384–390 (1981).
7. V.N. Krupchatnikov and L.I. Kurbatskaya, Atmos. Oceanic Opt. **13**, No. 8, 738–740 (2000).
8. R.G. Elingson, J. Ellis, and S. Feis, J. Geophys. Res. D **96**, No. 5, 8929–8953 (1991).
9. W.C. Wang, G.Y. Shi, and J.T. Kiehl, J. Geophys. Res. D **96**, No. 5, 9097–9103 (1991).